Inorg. Chem. **2005**, *44*, 9299–9304

First Experimental Evidence of Potassium Ordering in Layered $K_4Co_7O_{14}$

Maxime Blangero,[⊥] Rodolphe Decourt,[⊥] Dany Carlier,[⊥] Gerbrand Ceder,[†] Michael Pollet,[⊥] Jean-Pierre Doumerc,*[,⊥] Jacques Darriet,[⊥] and Claude Delmas[⊥]

Institut de Chimie de la Matière Condensée de Bordeaux, ICMCB-CNRS, 87, avenue du Dr. Schweitzer, 33608 Pessac Cedex, France, and Department of Materials Science and Engineering, Massachusetts Institute of Technology, 77 Massachusetts Avenue, Cambridge, Massachusetts 02139

Received August 30, 2005

The layered P2–$K_4Co_7O_{14}$ oxide has been prepared and characterized by means of X-ray diffraction, electrical conductivity, thermopower, and magnetic measurements. The crystal structure of $K_4Co_7O_{14}$ ($P6_3/m$ space group, $Z = 2$, $a = 7.5171(1)$ Å, and $c = 12.371(1)$ Å) consists of a stacking of slabs of edge-shared CoO_6 octahedra with K^+ ions occupying ordered positions in the interslab space, leading to a $a_0\sqrt{7} \times a_0\sqrt{7}$ supercell. Potential energy calculations at 0 K are in good agreement with the ordered distribution of potassium ions in the (*ab*) plane. This oxide is metallic, and the magnetic susceptibility is of Pauli-type, which contrasts with the Curie–Weiss behavior of the homologous Na_xCoO_2 ($x \approx 0.6$) oxide with close alkali content. The thermopower at room temperature is about one-third that of polycrystalline $Na_{0.6}CoO_2$.

Introduction

Layered cobaltite Na_xCoO_2 were intensively studied for more than 20 years as cathode materials for sodium batteries by Delmas et al.[1−3] In these works, the effect of oxygen nonstoichiometry on the electrochemical and transport properties was discussed. It is also this group who reported for the first time the high positive thermoelectric power up to 80 μV/K and low electrical resistivity of 3 mΩ·cm at 300 K for polycrystalline $Na_{0.7}CoO_2$ [3] as early as 1984. More recently, Terasaki et al.[4] put them back on stage as potential thermoelectric materials. They reported thermopower values as large as 100 μV/K, electrical resistivity of 0.2 mΩ·cm, and low thermal conductivity at 300 K for anisotropic $NaCo_2O_4$ single crystals. The origin of the large thermopower in this metallic-like conductor is still debated,[5−7] and interest was further stimulated in these oxides by the discovery of superconductivity below 5 K in $Na_{0.35}CoO_2{\cdot}1.3H_2O$.[8]

For the past few years, studies have dealt with various aspects of this system from ab initio calculations to structure and property analysis to explain its complex behavior. However, among the various questions regarding the behavior of Na_xCoO_2, the role played by the alkali metal is still unclear. With the exception of a few reports dealing with the observation of sodium ordering[9] or oxygen deficiency varying with the sodium[2,3] and eventually oxonium content,[10] very little is known about the possible contribution of ordering to the high figure of merit of this material. The role of intercalated water in the superconductive phase ($Na_{0.35}CoO_2{\cdot}1.3H_2O$) is still not definitely understood, as well.

In the present paper, we report the results of our preliminary study on the homologous potassium phase P2–K_xCoO_2. Using a full structure refinement, we give the first evidence for potassium ordering in the interslab space and discuss the properties of the new material as compared to the disordered phase and to the homologous sodium compounds.

* To whom correspondence should be addressed. E-mail: doumerc@icmcb-bordeaux.cnrs.fr. Fax: +00 33 5 40 00 83 73. Phone: +00 33 5 40 00 62 64.

[⊥] Institut de Chimie de la Matière Condensée de Bordeaux.

[†] Massachusetts Institute of Technology.

(1) Delmas, C.; Braconnier, J. J.; Fouassier, C.; Hagenmuller, P. *Solid State Ionics* **1981**, *3−4*, 165.
(2) Molenda, J.; Delmas, C.; Hagenmuller, P. *Solid State Ionics* **1983**, *9−10*, 431.
(3) Molenda, J.; Delmas, C.; Dordor, P.; Stoklosa, A. *Solid State Ionics* **1984**, *12*, 473.
(4) Terasaki, I.; Sasago, Y.; Uchinokura, K. *Phys. Rev. B* **1997**, *56*, 12685.
(5) Wang, Y.; Rogado, N. S.; Cava, R. J.; Ong, N. P. *Nature* **2003**, *432*, 425.
(6) Singh, D. J. *Phys. Rev. B* **2000**, *61*, 13397.
(7) Koshibae, W.; Maekawa, S. *Phys. Rev. Lett.* **2001**, *87*, 236603.
(8) Takada, K.; Sakurai, H.; Muromachi, E. T.; Izumi, F.; Dilanian, R. A.; Sasaki, T. A. *Lett. Nat.* **2004**, *422*, 53.
(9) Zandbergen, H. W.; Foo, M.; Xu, Q.; Kumar, V.; Cava. R. J. *Phys. Rev. B* **2004**, *70*, 024101.
(10) Bañobre-López, M.; Rivadulla, F.; Caudillo, M R.; López-Quintela, A.; Rivas, J.; Goodenough, J. B. *Chem. Mater.* **2005**, *17*, 1965.

10.1021/ic0514804 CCC: $30.25
Published on Web 11/11/2005

Experimental Section

Powder of K_xCoO_2 ($x = 4/7$) was obtained by a conventional solid-state reaction. KOH pellets and Co_3O_4 were finely mixed in a glovebox and put into a gold boat. Since by-produced K_2O is highly volatile, an empirical excess of KOH (17 wt%) is added. The resulting mixture was heated for 15 h to 600 °C under flowing dry O_2 and was subsequently slowly (1 °C/min) cooled to 300 °C. The dark-violet product was then taken out of the furnace and put immediately under dry argon atmosphere to prevent moisture contamination.

The XRD pattern of $K_4Co_7O_{14}$ was recorded on a Philips X'Pert Pro powder diffractometer in the Bragg−Brentano geometry, using Co Kα radiations. The data collections were made in the 10−120° 2θ range with a 0.0084° step, using an X'Celerator detector (linear PSD covering 2.122 mm). The powder was put in a specific airtight holder under dry argon to prevent any reaction with air moisture.

The diffraction data were analyzed using the Rietveld technique[11] as implemented in the Fullprof program.[12] Peak shape was described by a pseudo-Voigt function, and the background level was fitted with linear interpolation between a set of 90 given points with refinable heights.

Transport properties were measured on pellets sintered at 600 °C for 15 h, the compactness of which was close to 70%. Electrical DC conductivity measurements were performed with the four-probe method in the 4.2−300 K range. Thermoelectric power measurements were performed with a homemade equipment previously described.[13]

Zero field cooled (ZFC) and field cooled (FC) DC-magnetization data in an applied field up to 4 T were collected on a superconducting quantum interference device magnetometer (Quantum Design) in the 2−350 K temperature range.

The average oxidation state of cobalt, which is affected by the oxygen defect, δ, in $K_4Co_7O_{14-\delta}$, was determined by means of iodometric titration.[14]

The geometry optimization and energies calculations of different K/vacancy ordered cells with the P2 stacking were performed using density functional theory (DFT) in the spin-polarized generalized gradient approximation (GGA) with the projector augmented wave (PAW) method as implemented in the Vienna ab initio simulation package (VASP).[15] We chose a kinetic energy cutoff of 400 eV for the plane-wave basis and appropriate *k*-point mesh so that the total ground-state energy is converged to within 5 meV per K_x-CoO_2 formula unit.

Results and Discussion

1. Structure Determination. Delmas et al.[16] and Hoppe et al.[17] reported an approximated structure model of $K_{0.67}$-CoO_2 and $K_{0.55}CoO_2$, respectively, with space group $P6_3/mmc$ and subcell parameters close to $a \approx 2.8$ Å and $c \approx 12.3$ Å. Both models correspond to the P2 nomenclature[18] where the stacking along the *c* axis corresponds to two slabs of CoO_2 built up of CoO_6 octahedra sharing edges and where the potassium atoms are randomly distributed in prismatic sites in the interslab.

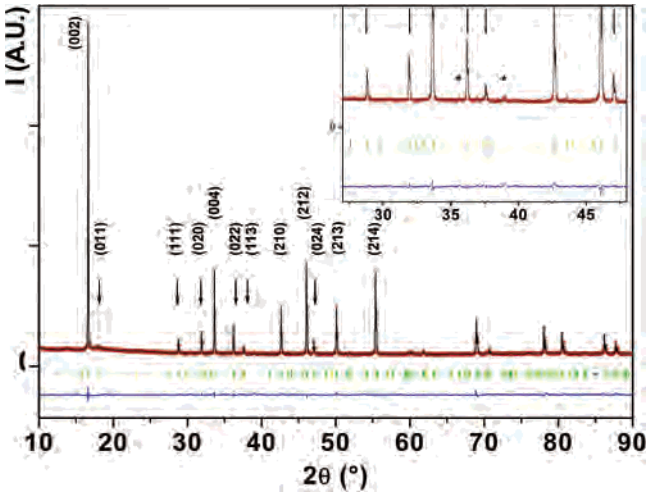

Figure 1. Rietveld refinement of the powder XRD pattern of $K_4Co_7O_{14}$ showing the superstructure. The observed (crosses), calculated (solid line), and difference (bottom line) profiles, as well as Bragg positions (vertical bars), are shown. Black arrows indicate the most intense reflections of the hexagonal supercell. The 90−120° 2θ range is not displayed for clarity. Inset: enlargement emphasizing the fit of the supercell reflections. * indicates peak positions of unreacted KOH,H_2O (JPDS 36-0791).

The powder X-ray diffraction pattern of $K_4Co_7O_{14}$ ($K_{4/7}CoO_2$) is obviously dominated by characteristic reflections of a P2 phase. Indeed, all the main peaks can be indexed in a hexagonal unit cell with $a_0 = 2.841$ Å and $c_0 = 12.371$ Å, very close to the values proposed for $K_{0.67}CoO_2$ ($a = 2.837(4)$ Å and $c = 12.26(2)$ Å). However, as shown in Figure 1, well-defined Bragg peaks (marked by an arrow) are not indexed using these parameters. The *d*-value positions of these nonindexed reflections clearly show that they do not result from any structural distortions due to a symmetry lowering of the unit cell. Indeed, no splitting of the peaks corresponding to the subcell is observed. In addition, the supercell does not correspond to a simple multiplication of the *c* parameter. To index the X-ray diffraction pattern, our strategy was to consider that the volume of the supercell (V) corresponds to an integer number time the elementary volume of the subcell (v). In the case of a hexagonal symmetry, the simplest possibilities are $V = 3v$ ($a_s = \sqrt{3}a_0$), $V = 4v$ ($a_s = 2a_0$), and $V = 7v$ ($a_s = \sqrt{7}a_0$).

All reflections could be successfully indexed in the hexagonal system on the basis of $P6_3/m$ space group with $a_s = \sqrt{7}a_0$ corresponding to the following hexagonal supercell parameters: $a_s = 7.517(1)$ Å and $c_s = 12.371(1)$ Å. Weak peaks in the 35−45° 2θ range (starred peaks) are attributed to the three strongest reflections of unreacted KOH excess in its hydrated form (JPDS 36-0791). The cell parameters of the supercell ($\mathbf{a}_s,\mathbf{b}_s,\mathbf{c}_s$) and the subcell ($\mathbf{a}_0,\mathbf{b}_0,\mathbf{c}_0$) are related through the matrix expression:

$$(\mathbf{a}_s,\mathbf{b}_s,\mathbf{c}_s) = (\mathbf{a}_0,\mathbf{b}_0,\mathbf{c}_0)\begin{bmatrix} 3 & -2 & 0 \\ 2 & 1 & 0 \\ 0 & 0 & 1 \end{bmatrix} \quad (1)$$

The corresponding (h,k,l) values of Bragg reflections are shown in Figure 1. The presence of the (111) and (113)

(11) Rietveld, H. M. *J. Appl. Cryst.* **1969**, *2*, 65.
(12) Rodriguez-Carvajal, J. *Physica B* **1993**, *192*, 55.
(13) Dordor, P.; Marquestaut, E.; Villeneuve G. *Rev. Phys. Appl.* **1980**, *15*, 1607.
(14) Tran, N.; Croguennec, L.; Jordy, C.; Biensan, P.; Delmas. C. *Solid State Ionics* **2005**, *176*, 1539.
(15) Kresse, G.; Furthmuller, J. *Comput. Mater. Sci.* **1996**, *6*, 15.
(16) Delmas, C.; Fouassier, C.; Hagenmuller, P. *J. Solid State Chem.* **1975**, *13*, 165.
(17) Jansen, M.; Hoppe, R. *Z. Anorg. Allg. Chem.* **1974**, *408*, 97.
(18) Fouassier, C.; Delmas, C.; Hagenmuller, P. *Mater. Res. Bull.* **1975**, *10*, 443.

Table 1. Structural Parameters of $K_4Co_7O_{14}$ from Rietveld Refinement Results at Room Temperature[a]

space group $P6_3/m$; $Z = 2$; theoretical density: 4.35						
conventional reliability factors of refinement						
cR_{wp}, 8.87%; cR_{exp}, 5.92%; χ^2, 2.24; R_{Bragg}, 3.60%						
hexagonal cell parameters (calculated)						
$a = 7.517(1)$ Å (7.5974 Å)			structural parameters		$c = 12.37(1)$ Å (12.426 Å)	
atom	site	x	y	z	U(Å^2)	SOF
Co1	2b	0	0	0	0.026(2)	1
Co2	12i	0.2862(4)	0.4289(5)	−0.0026(3)	=U(Co1)	1
O1	12i	0.2389(2)	0.1950(2)	0.0752(7)	0.018(2)	1
O2	12i	0.0976(1)	0.4759(2)	0.0753(5)	=U(O1)	1
O3	4f	1/3	2/3	−0.0832(2)	=U(O1)	1
K_f	2a	0	0	1/4	0.020(3)	1
K_e	6h	0.4436(5)	0.4143(5)	1/4	0.065(2)	1

[a] Calculated unit-cell parameters at 0 K are shown in parentheses.

reflections, which are forbidden for $P6_3/mmc$ indicates a change in the space group: the centrosymmetric space group compatible with these reflections and with the oxygen stacking of the P2 structure (ABBAAB...) is $P6_3/m$, which is a subgroup of $P6_3/mmc$. The atomic positions of cobalt and oxygen atoms have been deduced from eq 1: cobalt atoms are distributed in two independent positions, Co1 in the 2b site (000) and Co2 in the 12i site (xyz with $x \approx 1/4$, $y \approx 1/2$, and $z \approx 0$); the oxygen atoms occupy three positions, O1 and O2 in the 12i site (xyz) and O3 in the 4f site (1/3, 2/3, $z \approx 0$). A preliminary refinement using these positions leads to a R_{Bragg} value around 20% with all the atomic displacement parameter (ADP) fixed to a constant value of $U = 0.03$ Å^2. The difference Fourier map clearly shows that potassium atoms are only located in two positions: the first in the 2a site (0, 0, 1/4) for K_f and the second in the 6h site (x, y, 1/4) for K_e (where f and e subscripts stand, respectively, for oxygen octahedron face and edge sharing).

The structure refinement using the new positions leads for the conventional R-factors to $cR_{wp} = 8.87\%$, $cR_{exp} = 5.92\%$, and $R_{Bragg} = 3.60\%$. The observed and calculated diffraction profiles are drawn in Figure 1. The atomic positions are gathered in Table 1, and selected atomic bond distances in Table 2. A representation of the structure is given in Figure 2. The unit cell is built up by two slabs of edge-shared CoO_6 octahedra, which are rotated by 60° with respect to each other, and potassium atoms are crystallographically ordered in the interslab. The two potassium atoms (K_e and K_f) occupy prismatic sites with K−O distances ranging from 2.554 to 2.909 Å (Table 2). These K−O distances are in good agreement with those generally encountered for this atom.

Table 2. Selected Atomic Bond Distances According to Rietveld Refinement Results at Room Temperature[a]

Co1−Co2	×6	2.844(4) Å	(2.873 Å)
Co1−O1	×6	1.899(14) Å	(1.916 Å)
Co2−O1	×1	1.876(13) Å	(1.900 Å)
Co2−O1	×1	1.887(10) Å	(1.906 Å)
Co2−O2	×1	1.889(13) Å	(1.911 Å)
Co2−O2	×1	1.906(8) Å	(1.921 Å)
Co2−O2	×1	1.878(13) Å	(1.924 Å)
Co2−O3	×1	1.919(11) Å	(1.940 Å)
K_f−O1	×6	2.723(12) Å	(2.703 Å)
K_e−O1	×2	2.688(10) Å	(2.727 Å)
K_e−O2	×2	2.554(9) Å	(2.556 Å)
K_e−O3	×2	2.909(14) Å	(2.924 Å)
K_f−K_e	×3	3.230(4) Å	(3.321 Å)

[a] Calculated distances at 0 K are shown in parentheses.

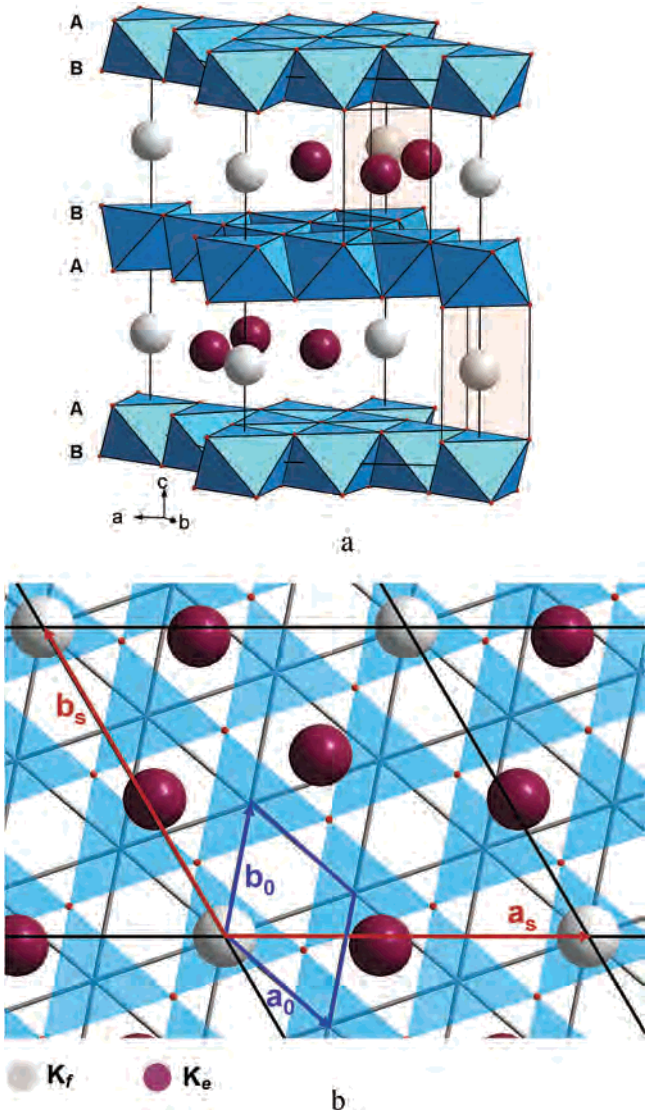

Figure 2. Crystal structure of P2-type $K_4Co_7O_{14}$ showing slabs of edge-shared CoO_6 octahedra and both types of coordination for potassium ions (K_e and K_f) (a). The projection of the structure along the c axis displaying the Co triangular array ($z = 1/2$) as lines, K atoms ($z = 3/4$) as spheres, and between the upper face of CoO_6 octahedra as filled triangles, and shows the ordering of K ions and the shifted position of K_e ones from the prism center (b).

The potassium ions, on two crystallographically distinct sites, are trigonal prismatic in coordination to the oxygen atoms and differ in their coordination with CoO_6 octahedra: K_fO_6 prisms share faces with CoO_6 octahedra; whereas K_eO_6 prisms share edges with CoO_6 octahedra (Figure 2). The Co−O distances are close to the values reported for Na_x-CoO_2 [19] (∼1.90 for $x = 0.5$), and very similar within the two cobalt sites (Table 2). As a consequence, cationic ordering observed in $K_4Co_7O_{14}$ could hardly be driven by a charge ordering between Co^{3+} and Co^{4+} in the two independent positions, in good agreement with the metallic character of the material.

The P2−K_xCoO_2 system has also been theoretically investigated, performing first principles calculations, and we report here the preliminary results concerning more specifically the $x = 4/7$ composition.

Calculations of the site energy at low potassium concentration ($x = 1/14$ in K_xCoO_2) indicate that the K_e site (that does not share any face with CoO_6 octahedra) is substantially more stable than the K_f one by 112 meV. Therefore, all the potassium ions are expected to be located in the K_e sites. However, we find that when we optimize a $a_0\sqrt{7} \times a_0\sqrt{7}$ cell with the K^+ ions located only in the K_e sites at composition $x = 4/7$ some of them spontaneously leave their site to occupy K_f-type sites This can be understood as a balance between the site energy and electrostatic energy. Occupying the K_f sites allows for larger K−K distances, thereby minimizing the electrostatic K^+-K^+ repulsion. Similar effects were considered to explain the calculated ground state orderings in the T#2−Li_xCoO_2 [20] and the P2−Na_xCoO_2 [21] systems where different alkaline sites are available.

Among the different potassium/vacancy orderings tested for the $a_0\sqrt{7} \times a_0\sqrt{7}$ cell and the $x = 4/7$ potassium concentration, the ground-state optimized structure obtained is in good agreement with the experimental one (Tables 1 and 2). The cell parameters and ion distances are well reproduced by the calculation. The distribution of the K_e−O distances clearly shows that the electrostatic K^+-K^+ repulsion is strong enough to displace the ions from the center of their prisms. A close similarity of the refined and calculated structure parameters is noticed.

2. Physical Properties. 2.1. Magnetic Properties. $K_4Co_7O_{14}$ shows an almost temperature-independent paramagnetic susceptibility (450×10^{-6} emu/mol at 350 K). The susceptibility slightly increases below 20 K, which could be attributed to some paramagnetic impurities (Figure 3). Two main contributions to the magnetic susceptibility can be considered, a Pauli-type contribution from the itinerant carriers possibly enhanced by electronic correlations and a second-order Van Vleck contribution originating from electrons localized on Co^{3+} ions (∼100×10^{-6} emu/mol).[22] The

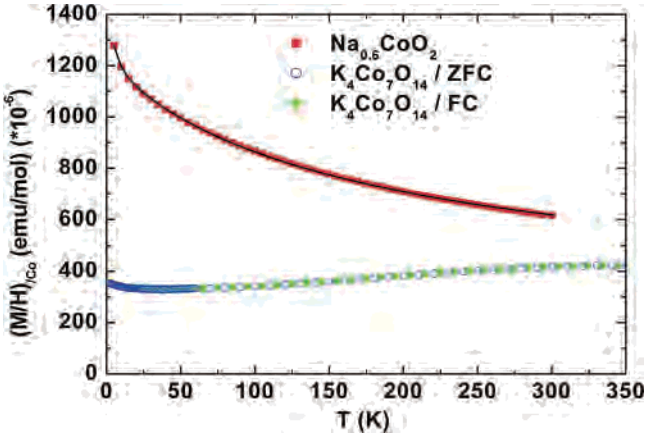

Figure 3. Magnetic susceptibility per Co ion for $Na_{0.60}CoO_2$ (solid squares) and for ZFC (open circles) and FC (solid circles) $K_4Co_7O_{14}$. For $Na_{0.6}$-CoO_2, it fits $\chi(T) = \chi_0 + C_1/(T + \theta_p) + C_2/T$, with $\theta_p = -180(1)$ K, $\chi_0 = 280(1) \times 10^{-6}$ emu/mol, $C_1 = 0.161(1)$ emu·K/mol, and $C_2 = 0.0006(1)$ emu·K/mol. The C_2/T term can be attributed to the paramagnetic contribution of an unknown impurity. The C_1 Curie constant agrees with an atomic concentration of low-spin Co^{4+} of 42% in good agreement with the nominal composition.

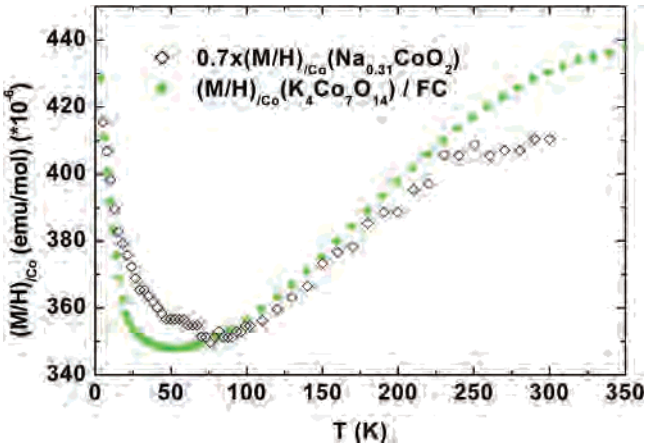

Figure 4. Magnetic susceptibility per Co of $Na_{0.31}CoO_2$ single crystals (magnified scale for clarity (×0.7)) (open squares) reported by Foo et al.[23] and of polycrystalline $K_4Co_7O_{14}$ (solid circles).

disordered potassium cobaltite displays a similar magnetization curve (not shown). Such a behavior differs from that of Na_xCoO_2 ($x \approx 0.6$) obtained under similar conditions (Figure 3). The sodium compound exhibits Curie−Weiss behavior with a temperature-independent term of 280×10^{-6} emu/mol and a Curie constant denoting full spin polarization. As shown with a magnified scale in Figure 4 (different scales for clarity), the K-ordered compound presents a behavior closer to that of $Na_{0.31}CoO_2$ (according to the measurements of Foo et al.)[23] rather than $Na_{0.6}CoO_2$. Although the magnified scale shows a significant increase of the magnetization below ca. 10 K, no conclusion about any magnetic long-range ordering, magnetic fluctuations, or spin density wave can definitely be drawn at the present stage of our investigations.

2.2. Electrical Resistivity. Figure 5 shows the electrical resistivity measurements for polycrystalline $K_4Co_7O_{14}$. It

(19) Huang, Q.; Foo, M. L.; Lynn, J. W.; Zandbergen, H. W.; Lawes, G.; Wang, Y.; Toby, B. H.; Ramirez, A. P.; Ong, N. P.; Cava, R. J. *Condens. Matter* **2004**, *32*, 5803.
(20) Carlier, D.; Van der Ven, A.; DelmasC.; Ceder, G. *Chem. Mater.* **2003**, *15*, 2651.
(21) Zhang, P.; Capaz, R. B.; Cohen, M. L.; Louie, S. G. *Phys. Rev. B* **2005**, *71*, 153102.
(22) Mabbs, F. E.; Machin, D. J. *Magnetism and Transition Metal Complexes*; Chapman Hall: London, 1973.
(23) Foo, M. L.; Wang, Y.; Watauchi, S.; Zandbergen, H. W., He, T.; Cava, R. J.; Ong, N. P. *Phys. Rev. Lett.* **2004**, *92*, 247001.

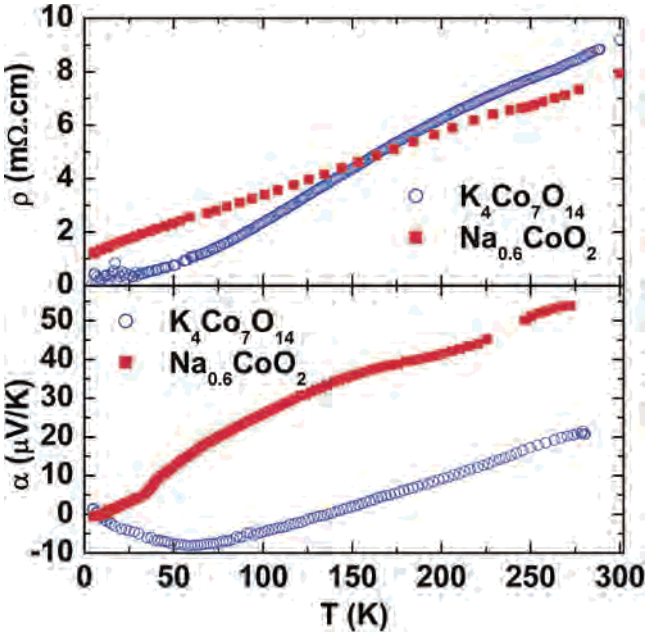

Figure 5. Temperature dependence of the thermopower and of the electrical resistivity measured on sintered pellets for both $K_4Co_7O_{14}$ (open circles) and $Na_{0.6}CoO_2$ (filled squares).

monotonically decreases with decreasing temperature, indicating a metallic-like behavior with a change from a phonon scattering regime above 60 K to quasi-elastic scattering below 60 K. The high values of resistivity are presumably ascribed to the low bulk density of the sample and to the size of the grains insufficiently grown at low sintering temperature. The behavior of the K-disordered cobaltite (not shown) exhibits the same trend with similar temperature dependence and inflection near 135 K; the main difference lies in the magnitude of the electrical resistivity, which is shifted to higher values in the K-disordered compound with a monotonic decreasing offset from ~7.5 mΩ·cm at 300 K to 2 mΩ·cm at 4.2 K. A shorter elastic mean free path in the later phase could simply result from the random distribution of K^+ ions that creates random fluctuations of the carrier potential energy.

More interesting is the comparison with the sodium cobaltites: first, we can notice that the resistivity values (Figure 5) have the same order of magnitude as for polycrystalline Na_xCoO_2 ($x \approx 0.6$). These layered compounds are highly anisotropic, and it is well known that the measurements on polycrystalline samples generally reflect the behavior in the (*ab*) plane rather than along the *c* axis;[4] owing to the literature data on both single crystals and polycrystalline samples in homologous sodium compounds, one can reasonably expect a high electrical conduction through the CoO_2 planes (~few tenths Ω·cm) in $K_4Co_7O_{14}$. The main distinctive feature stands in the temperature dependence of the Na and K compounds (whether ordered or not): the low-temperature behavior is typically metallic in the case of $K_4Co_7O_{14}$, while $Na_{0.6}CoO_2$ exhibits no residual resistivity down to 4 K; similar behavior has already been discussed by Rivadulla et al.[24] and ascribed to a departure from the conventional metallic behavior of a 3D electron gas due to strong correlation effects. For Na_xCoO_2 single

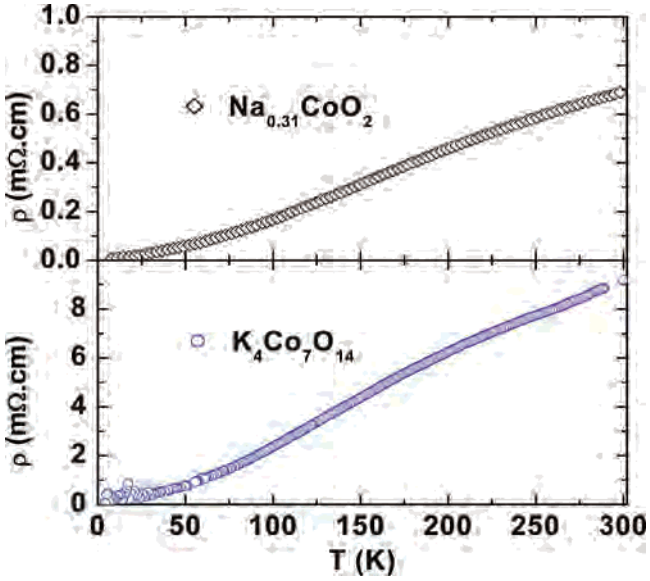

Figure 6. Temperature dependence of the electrical resistivity measured on sintered pellets for $K_4Co_7O_{14}$ (open circles) and in the (*ab*) plane for $Na_{0.31}CoO_2$ (open squares) reported by Foo et al.[23]

crystals, the conductivity along the *c* axis becomes thermally activated above ca. 170 K[24] as the Co−O−O−Co interactions are decreasing in this direction upon thermal expansion. Comparing the Co−Co interactions on the basis of the Co−Co distances in and out of the plane at room temperature clearly shows that, for the same alkali doping rate, these interactions are much weaker in the K compound, especially along the *c* axis. The Co−Co distances in the (*ab*) plane are slightly increased from 2.825 to 2.841 Å ($\Delta a \approx 0.5\%$) and noticeably increased along the *c* axis from 5.490 to 6.213 Å ($\Delta c \approx 13\%$) for Na and K compounds, respectively.

Actually, the behavior of $K_4Co_7O_{14}$ is closer to that of Na_xCoO_2 ($x \approx 0.31$),[23] the precursor of the superconductive hydrated sodium cobaltite[8] (Figure 6). This last phase also exhibits a high *c*/*a* ratio (~4 vs ~4.35 for $K_4Co_7O_{14}$) (*a* refers to the subcell parameter a_0 for $K_4Co_7O_{14}$). The main difference between the two compounds lies in the doping level which controls the oxidation state of the cobalt. However, Bañobre-López et al. have clearly shown that the oxygen stoichiometry can be strongly lowered in the sodium compound and that, for $x < 0.5$, the Co^{3+}/Co^{4+} atomic ratio is even larger than 50%.[10] In particular, their measurements in $Na_{0.31}CoO_2$ shows that $\%Co^{3+} = 57\%$, while a linear extrapolation of their data for $x = 4/7$ leads to $\%Co^{3+} = 75\%$. Our measurements carried out in $K_4Co_7O_{14-\delta}$ using a similar iodometric titration method lead to $\delta < 0.2$ giving a $\%Co^{3+} < 63\%$. This upper limit is justified by the presence of traces of KOH in the sample as shown on XRD patterns (Figure 1, inset); these traces could hardly be washed out without impairing the sample. The average oxidation state of the cobalt ion in $K_4Co_7O_{14}$ then obviously appears closer to the one of low-doped sodium cobaltites rather than the one of $Na_{0.6}CoO_2$. This result tends to show that, whatever the nature of the alkali ion, the *T* trend of the resistivity seems

(24) Rivadulla, F.; Zhou, J. S.; Goodenough, J. B. *Phys. Rev. B* **2003**, *68*, 075108.

mainly governed by the oxidation state of the cobalt ion whereas only the magnitude of the resistivity seems weakly changed.

2.3. Thermoelectric Power. The Seebeck coefficient shows a complex behavior (Figure 5). The thermopower is positive between 4.2 and 7 K and from 135 K to room temperature. It features a somewhat T^2 dependence from 7 to 80 K, with a negative minimum at 57 K and a linear dependence from 80 K to room temperature as expected for a typical metal. Except for the lowest-sign reversal temperature, this behavior offers the same trend than the one previously reported by Delmas et al. for a disordered $K_{0.67}CoO_2$.[16] However, the characteristic temperatures for the different regimes are lowered in the case of $K_4Co_7O_{14}$, as is the magnitude of the thermopower. This could be ascribed to either the lower K content, the K ordering, or both. However, for the disordered phase, the moisture sensitivity of the sample prevents us from recording data reliable enough for further discussing this point (to prevent this problem, we are now focusing on the growth of single crystals for which the water sensitivity seems to be lower, according to preliminary results). One can notice that the sign reversal close to 135 K in $K_4Co_7O_{14}$ occurs at the same temperature as an inflection in the conductivity plot. This sign reversal takes place in a temperature range where the thermopower follows the linear variation previously described precluding any major change in the structure (atomic or magnetic), and it is more likely to be described as a second-order transition or a simple continuous evolution of some property. Both this feature and the low-temperature one are still under investigation, and we still have no clear explanations for them. We can still notice for comparison purpose that the observed behavior is very far from that of $Na_{0.6}CoO_2$ and that the magnitude of the thermopower is also much lower (Figure 5). Assuming that the large value of the thermopower in $Na_{0.6}CoO_2$ is due to spin entropy as suggested previously,[5] the important difference of behavior between the Na and K cobaltite can be correlated with their magnetic properties discussed above. Whereas $Na_{0.6}CoO_2$ exhibits a CW behavior for which a large spin entropy contribution can be expected in the paramagnetic state, the potassium cobaltite, on the other hand, presents a Pauli-type behavior for which a significant spin contribution to α can hardly be expected. Nevertheless, for $K_4Co_7O_{14}$, the value of α at room temperature remains relatively large compared to that of a "classical" metal. Two effects can account for this enhanced thermopower: (i) strong electron−electron correlations and (ii) a particular shape of the dispersion curves near the Fermi level arising from the 2D character of the Co sublattice and to the possible overlap of the e and a_1 orbitals resulting from the splitting of the t_{2g} orbitals, the degeneracy of which is lifted by the trigonal crystal field due to the compression of the octahedra along the 3-fold axis taken parallel to the *z* direction.

Conclusion

The crystal structure of $K_4Co_7O_{14}$ consists of P2-type stacking of edge-shared CoO_6 octahedra slabs between which K^+ ions occupy ordered positions giving rise to a $a_0\sqrt{7} \times a_0\sqrt{7}$ supercell ($Z = 2$, SG: $P6_3/m$). Potential energy calculations at 0 K agree well with the ordered distribution of potassium deduced from the structure refinement. The oxide is metallic, and the magnetic susceptibility is of Pauli-type. The electrical conductivity is enhanced through the K ordering. Its magnitude is of the same order than the conductivity of $Na_{0.6}CoO_2$. However, the Co−Co interactions along the *c* axis are lowered in the K compound due to the increase of the Co−O−O−Co distances, enhancing the 2D character of the system. This effect accounts for a large difference in the temperature dependence of the electrical conductivity below 50 K: whereas for the K cobaltite a residual resistivity is normally observed at low temperature as the phonon diffusion length becomes longer than the (elastic) mean free path, for $Na_{0.6}CoO_2$, the conductivity is monotonically decreasing as *T* decreases, at least down to liquid helium temperature. Actually, the electrical and magnetic behaviors of $K_4Co_7O_{14}$ are closer to those of Na_xCoO_2 oxides having a much lower alkali concentration ($x < 0.5$). Such a behavior is ascribed to an oxygen deficiency much smaller for the K cobaltite than for the Na one, as confirmed by chemical analysis, and resulting in close average oxidation states of cobalt in both oxides. The behavior of $K_4Co_7O_{14}$ is close to that of the precursor of the hydrated superconducting sodium cobaltite, and further studying the K system should bring a better understanding of the origin of superconductivity in these materials. In this context, we now focus on the whole K_xCoO_2 phase diagram and on the effects of water intercalation in some selected compounds.

Acknowledgment. The authors (M.B., D.C., M.P., J.P.D., J.D., C.D.) thank Région Aquitaine and CNRS for financial support and C. Denage (ICMCB-CNRS) for technical assistance. D.C. wishes to thank the Du Pont de Nemours Company for financial support. G.C. acknowledges support from the Department of Energy under Contract No. DE-FG02-96ER45571.

IC0514804